Article

Analysis of Curing and Mechanical Performance of Pre-Impregnated Carbon Fibers Cured within Concrete

Martin Scheurer [1,*], Matthias Kalthoff [2], Thomas Matschei [2], Michael Raupach [2] and Thomas Gries [1]

1   Institut für Textiltechnik, RWTH Aachen University, 52062 Aachen, Germany
2   Institute of Building Materials Research (IBAC), RWTH Aachen University, 52062 Aachen, Germany
*   Correspondence: martin.scheurer@ita.rwth-aachen.de

Abstract: In carbon-reinforced concrete, the commonly used steel reinforcement is replaced with carbon fiber reinforcement textiles, enabling thin-walled elements by using new construction principles. The high drapability of textiles offers design opportunities for new concrete structures. However, commonly utilized textiles are impregnated with comparatively stiff polymeric materials to ensure load transmission into the textile, limiting drapability. In this paper, a new approach is analyzed: the use of pre-impregnated textiles cured within the concrete matrix. This enables the production of filigree, highly curved components with high mechanical performance, as needed for novel additive manufacturing methods. In the presented trials, rovings were successfully impregnated with potential impregnation materials, cured within the concrete, and compared to rovings cured outside of the concrete. The analysis of the curing process using a rolling ball test determines that all materials have to be placed in concrete 4 to 24 h after impregnation. The results of uniaxial tensile tests on reinforced concrete show that maximum load is increased by up to 87% for rovings cured within concrete (compared to non-impregnated rovings). This load increase was higher for rovings cured outside of concrete (up to 185%), indicating that the concrete environment interferes with the curing process, requiring further analysis and adaptation.

Keywords: carbon-reinforced concrete (CRC); textile-reinforced concrete (TRC); reinforcement textile; carbon; coating; prepreg

1. Introduction

The construction and building sector has one of the largest resource usage footprints of all industries, being responsible for about 50% of the use of extracted materials and energy in the European Union [1]. In addition, the sector causes approximately one-third of the greenhouse gas emissions in the European Union [2,3], with the global production of cement alone accounting for about 8% of global greenhouse gas emissions [4]. One key challenge in industry and research is the reduction of this resource usage and greenhouse gas emissions, with several potential solutions being investigated [5–12].

One possible solution to reduce concrete (and, therefore, cement) usage is the substitution of conventional steel reinforcement with high-performance technical textiles [13]. This method is known as textile-reinforced concrete (TRC), sometimes called textile-reinforced mortar (TRM) or fabric-reinforced cementitious matrix (FRCM) [14,15]. Since the technical textile does not corrode when in contact with oxygen, the necessary concrete cover of the reinforcement can be reduced to a minimum [14,16]. Depending on the building design and resulting loads, concrete usage and greenhouse gas emissions can be reduced significantly [17–19]. The main advantage of this method is reduced concrete usage and the very high mechanical performance of the final component. However, concrete mixes need to be adapted for use with textiles. The processing methods to produce the concrete elements need to be adapted as well since the handling of textiles differs from the handling of steel grids [14,20].

Commonly, textiles used for concrete reinforcement are impregnated with a polymer material [16,21] or mineral dispersion [22–24] to ensure proper load induction into the fibers of the reinforcement textile. Uncoated textiles often fail in a so-called pullout failure, since the comparatively coarse concrete matrix does not penetrate the textile and the inner filaments do not contribute to load bearing [25]. In addition to the load induction, coatings also improve the durability of the reinforcement textiles by protecting against the alkaline concrete environment and by improving handling during production [16,21].

Usually, textiles are impregnated immediately after textile production and the impregnation material is immediately cured [21]. This results in comparatively stiff textiles, which offer high mechanical performance with good bond strength with the concrete matrix, but limited drapability of the cured textile, resulting in limited design flexibility. Current impregnation materials do not allow for high design flexibility and high mechanical performance at the same time [26].

One focus of current research is the additive manufacturing of filigree and curved textile-reinforced concrete components, which are designed to be load-bearing [27]. Innovative processes such as 3D concrete printing [28,29] and concrete extrusion [30,31] are used to realize these components. In order to be able to use these processes, high and, at the same time, contradictory demands are placed on the reinforcement used, which must be both flexible and have high tensile strength. For the production of these load-path optimized carbon-reinforced concrete structures, small bending radii are necessary, which can currently only be realized with non-impregnated textiles, and, at the same time, the textile must absorb the high tensile forces, as is the case with impregnated hardened textiles. To meet these requirements, the textiles must be integrated into the concrete printing or extrusion process in their freshly impregnated state. This type of implementation has not yet been sufficiently researched. Closing this research gap is the goal of this paper.

In this paper, a novel approach for impregnation materials for textile reinforcements for concrete is investigated. In this approach, the textile is impregnated as usual, but the curing of the impregnation material happens after placing the impregnated textile in the concrete matrix. This allows for a highly flexible, drapable textile enabling the design freedom necessary for new applications and additive manufacturing methods, such as 3D concrete printing or concrete extrusion, while, at the same time, promising high mechanical performance of the finished composite. If successfully incorporated, this approach would close a knowledge gap preventing the economic use of textile-reinforced concrete for free-formed structural applications.

In this work, different materials are investigated and tested regarding impregnation quality, bending stiffness, curing speed, and performance within the concrete. The results show that full impregnation is possible with all tested materials and that all tested materials cure within 24 h of impregnation. Most materials improve the mechanical performance of the textile within the concrete when using the new approach of curing within the concrete, but the load bearing is increased even further when the impregnated textiles are cured prior to placement within the concrete.

2. Materials and Methods

This section describes the materials and methods used in this paper. The materials are namely the textiles/rovings, the concrete mix, and the impregnation materials. The methods refer to the impregnation method as well as the test setups to determine the bending stiffness, the progress of the curing of the impregnation materials, and the mechanical testing.

2.1. Materials

Within the scope of this work, carbon rovings of the type Tenax™-E STS40 E23 24K by Teijin Carbon Europe GmbH, Wuppertal, Germany were used. Some specifications of the rovings, according to the manufacturer, are given in Table 1.

Table 1. Selected properties of the used carbon rovings Tenax™-E STS40 E23 24K according to the manufacturer [32].

Titer [tex]	Tensile Strength [MPa]	Young's Modulus [GPa]	Elongation at Break [%]	Filament Diameter [μm]	Sizing Content [%]
1600	4300	250	1.7	7.0	1.3

Table 2 lists the mixture design of the concrete mix used for the production of textile-reinforced concrete test specimens in this work. This mixture was adapted for use in a laminating process as needed for the production of test specimens in this work and is based on a mixture used in concrete extrusion to enable rapid transfer to additive manufacturing of concrete components [30].

Table 2. Mixture design of the concrete mix used in this work, based on [30].

Ingredient	Amount [kg/m^3]
CEM I 42.5 R	620
Fly ash	113.6
Sand 0.1–0.5 mm	552.3
Quartz powder 0–0.250	530
Silica fume powder	36
Water	319.3
PCE super-plasticizer	2.5

Table 3 lists the impregnation materials used in the scope of this study as well as selected properties according to the respective manufacturer data sheets. The materials were selected based on a screening of potential, commercially available materials that had previously been used in similar applications (e.g., with concrete or for reinforcement textiles).

Table 3. Impregnation materials used in this work.

Resin	Curing Agent	Designation in This Work	Dynamic Viscosity [mPa*s]	Density at 23 °C [g/cm^3]
Bisphenol A/F resin	Polyetherdiamine	Epoxy resin	200–400	1.15
Watery dispersion of carboxylated styrene-butadiene-copolymers	Etherified methylolmelamine-solution	Styrene-butadiene-rubber dispersion	1000	1.02
Water-dispersed epoxy resin	Amine polymer	dispeler-dispersed epoxy resin	250	1.05
Anionic polycarbonate polyurethane dispersion	Hydrophilic, aliphatic polyisocyanate based on hexamethylene-diisocyanate	Polycarbonate polyurethane dispersion	1400 [1]	1.05

[1] without hardener.

2.2. Methods

All impregnation materials were mixed according to manufacturer specifications prior to the impregnation of the fibers. The rovings were impregnated using a Labcoater EA210 by Coatema Coating Machinery GmbH, Dormagen, Germany. This machine uses a discontinuous impregnation method allowing for the simultaneous impregnation of multiple rovings using only a small amount of impregnation material. The machine and the impregnation process are shown in Figure 1.
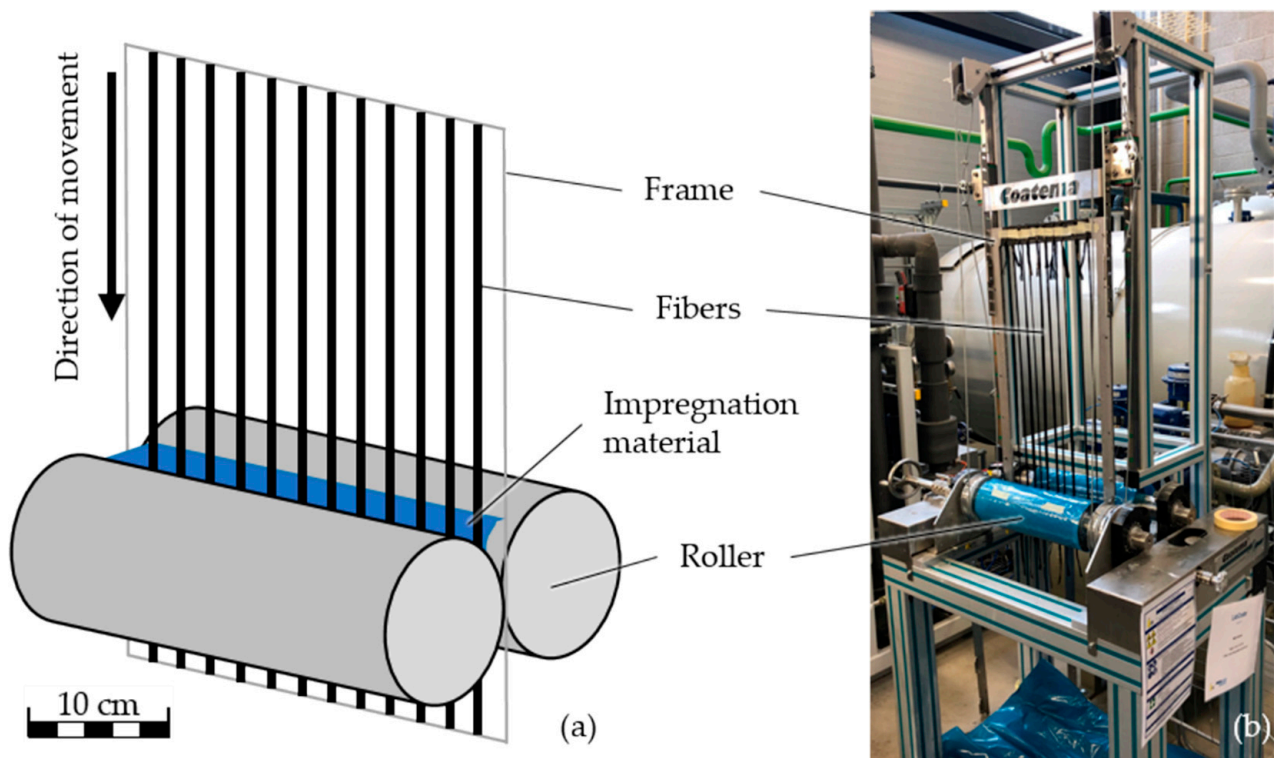
Figure 1. Representation of the discontinuous impregnation method used in this work: (**a**) schematic representation; (**b**) picture.

Prior to impregnation, the rovings are fixed onto a metal frame, which is placed in between the rollers of the Labcoater. The impregnation material is then poured in between the rollers and the rovings are moved through the rollers vertically. On the downward motion, the impregnation material is moved into the rovings, and on the upward motion, the excess coating material is removed from the rovings. Based on pretests, the clearance between the rollers was set to 0.7 mm and the applied pressure of the rollers was set to 6 bar. To ensure full impregnation of the fibers, the quality of the impregnation was checked using light microscopy. With the settings specified above, full impregnation could be achieved with all four materials specified in Table 3.

To determine the drapability of the impregnated rovings, a modified cantilever test adapted from the one described in DIN 53362 [33] was used. The impregnated rovings were cut to a length of 60 cm, weighted, and their width determined. The rovings were then placed on the measuring device and pushed over the edge using a slider until an overhang of 50 cm was reached. Then, the deflection of the tip of the roving was measured. The ordinary cantilever test described in DIN 53362 uses the length at which the textile intersects with the measurement plane at an inclination of 41°30′. Since the cured textiles were too stiff to intersect with this plane, even after increasing the size of the measurement apparatus, deflection at the tip of the roving was measured instead. The test setup is shown in Figure 2.
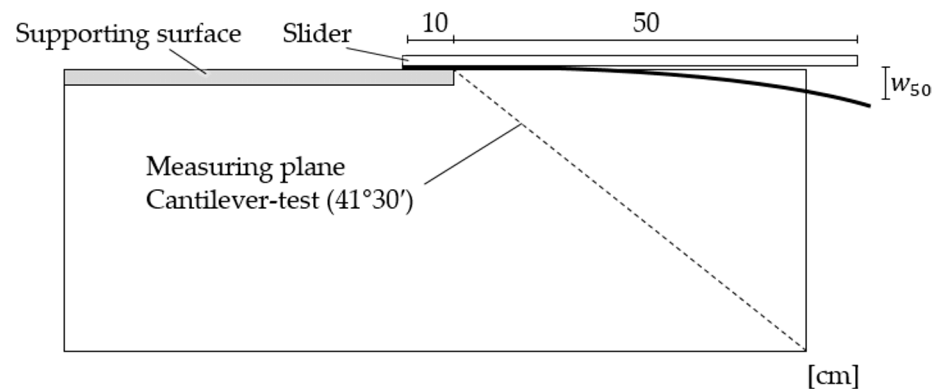
Figure 2. Schematic representation of the adapted Cantilever test used in this work.

To evaluate the curing of the impregnation materials over time, a rolling ball test based on [34,35] was used. In this method, a steel ball is rolled from a ramp onto the surface that is tested. The rolling ball test is used to measure the tack of textiles impregnated with the materials given in Table 3 at different points in time after impregnation (1 min, 5 min, 10 min, 30 min, 1 h, 4 h, 10 h, 24 h, and 48 h). Since the measurement of the tack of single rovings is difficult, a warp-knit textile was used instead. The textile was impregnated using the Labcoater as described above. Since the Labcoater limits the length of the textile that can be impregnated, the rolling ball sometimes traveled across the whole textile, rendering the measurement invalid. Therefore, the length of the ramp used was reduced to 10 cm. The final test setup is shown in Figure 3.
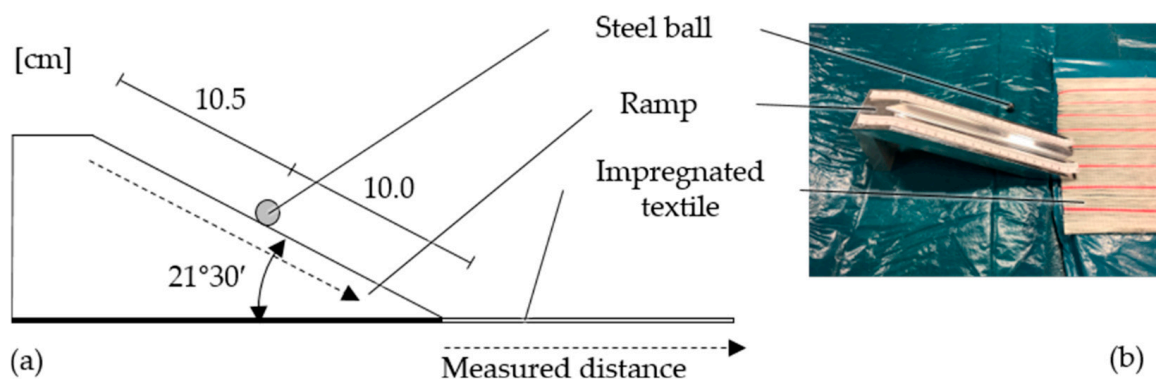

Figure 3. Representation of the rolling ball test used in this work: (**a**) schematic representation; (**b**) picture.

To evaluate the mechanical performance of the textile-reinforced concrete composite, uniaxial tensile test specimens based on the recommendations in [36] were produced. Corresponding to the recommendation [36], the dimensions of the uniaxial tensile test specimens were $600 \times 50 \times 10 \text{ mm}^3$, with each specimen containing four carbon rovings spaced equidistant and placed in the middle of the specimen thickness. Specimens were produced in a laminating process using the concrete specified in Table 2 in molds in which the rovings were clamped at the right positions. Two variations of specimens were produced for each impregnation material: one in which the impregnated rovings were cured prior to embedding in the concrete (called fresh-on-hard, FoH) and one in which the impregnated roving was embedded in an uncured state and cured within the concrete (called fresh-on-fresh, FoF). In addition, one series with uncoated rovings was produced as a baseline comparison. Figure 4 shows the tensile test specimen dimensions and production process. Tests were performed after a curing of the concrete for 14 days.

Specimen dimensions
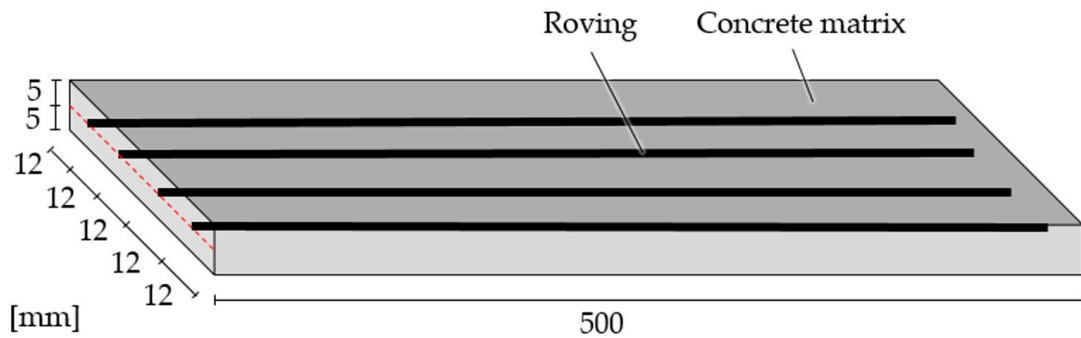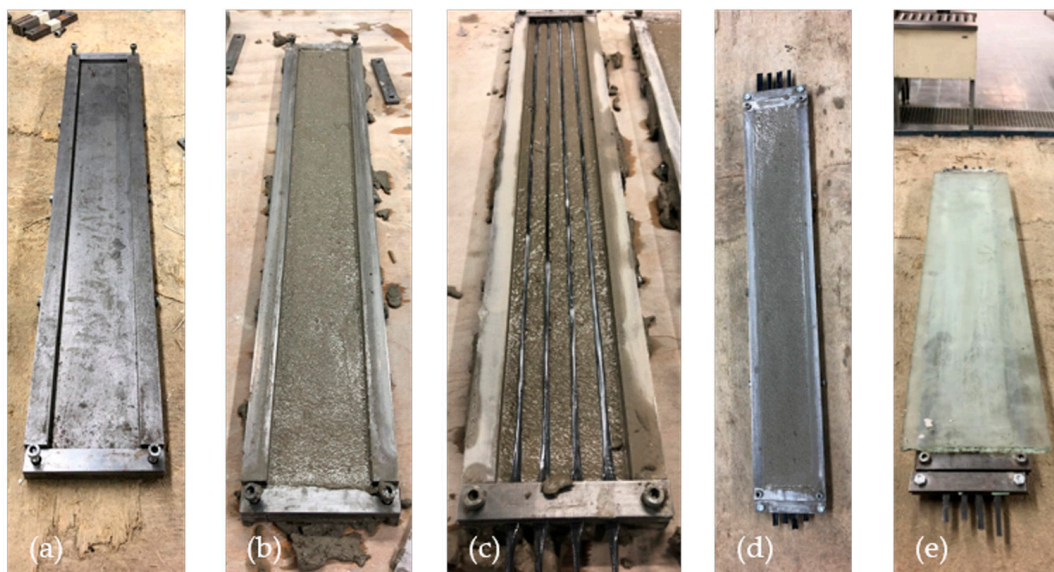

Specimen production process

Figure 4. Representation of the tensile test specimens used in this work and their production process. Top: specimen dimensions; Bottom: production process: (**a**) clean mold; (**b**) first concrete layer; (**c**) placement of rovings; (**d**) second concrete layer; (**e**) placement of glass plate on top to ensure a smooth surface for clamping.

Tensile tests were performed on a tensile testing machine type Zwick 1464 (ZwickRoell GmbH & Co. KG, Ulm, Germany). To ensure load induction, both ends of the tensile test specimens were clamped using steel plates at a length of 125 mm on each end. Elastomer strips were placed in between the steel plates and the specimens to offset any unevenness in the surface and to improve load induction. The steel plates were clamped using six screws each, which were tightened with a torque of 5 Nm. To measure the strain, measuring devices type Strain Link 2.5 mm by Hottinger Baldwin Messtechnik GmbH, Darmstadt, Germany, were fixed onto both sides of each specimen. The test speed was 2 mm/min. The final test setup is shown in Figure 5.
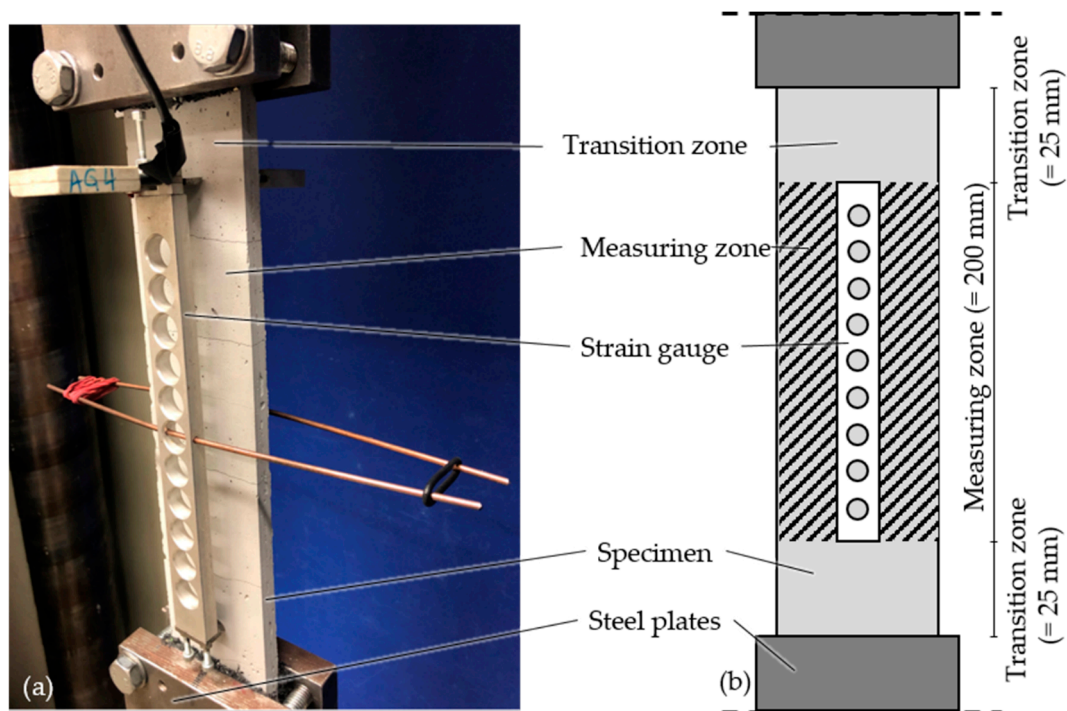
Figure 5. Representation of the tensile test setup used in this work: (**a**) picture; (**b**) schematic representation.

3. Results and Discussion

This section provides and discusses the results obtained from the tests specified above.

3.1. Cantilever Tests

The bending stiffness of impregnated and cured rovings is evaluated using the cantilever test described above after at least 24 h. Table 4 lists the deflection of each specimen as well as the average deflection for each coating.

Table 4. Results of the cantilever tests.

Impregnation Material	Specimen Number	Deflection [cm]	Average Deflection [cm]
Epoxy resin	1	1.8	
	2	1.9	1.93
	3	2.1	
Styrene-butadiene-rubber dispersion	1	2.5	
	2	3.0	2.93
	3	3.3	
Water-dispersed epoxy resin	1	3.1	
	2	3.5	3.83
	3	4.9	
Polycarbonate polyurethane dispersion	1	2.1	
	2	1.9	2.13
	3	2.4	

Modeling the roving as a cantilever arm enables the calculation of the bending stiffness of rovings impregnated with each material. The resulting formula is:

$$EI = \frac{g \times M \times b \times 10^{-3} \times l_o^{3}}{3 \times w_{50}} \tag{1}$$

with EI being the bending stiffness in $N*cm^2$, g being the acceleration due to gravity (9.81 m/s^2), M being the mass per area in g/m^2, b being the specimen width in cm, l_o being the overhang length in cm, and w_{50} being the deflection at the tip of the roving in cm. The bending stiffness of each material is compared in Figure 6. The full table of all measurements used for this calculation is given in Appendix A (Table A1).
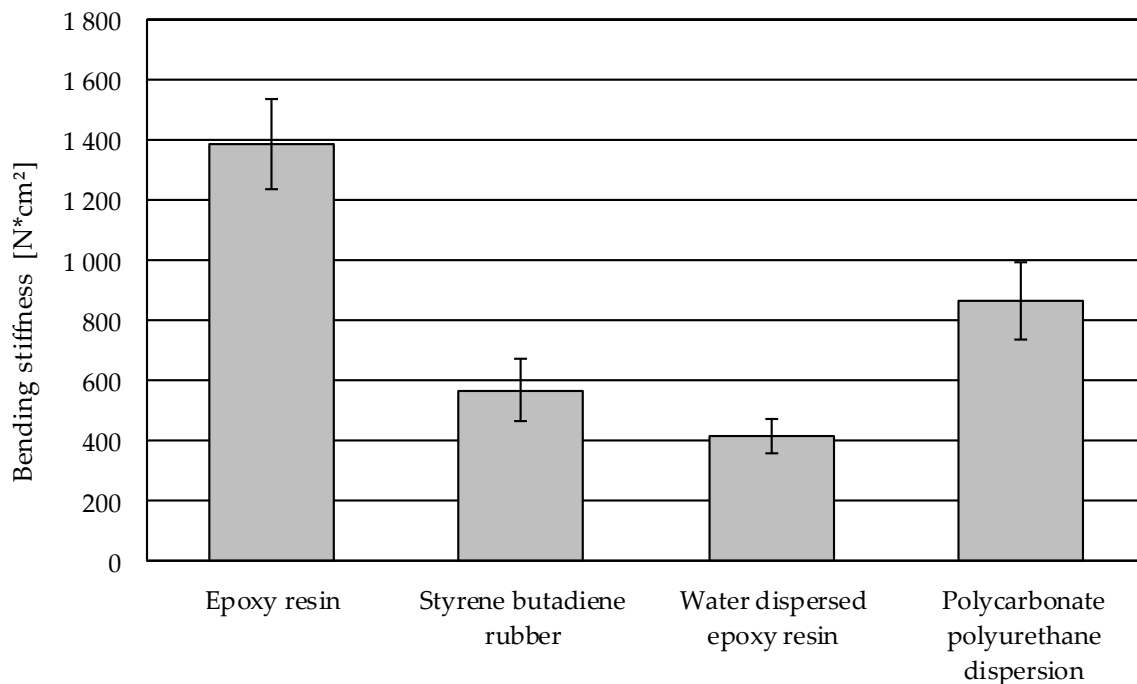

Figure 6. Resulting average bending stiffness of cured impregnated rovings in the cantilever tests (error bars indicate standard deviation).

The obtained results show that, as expected, rovings impregnated with epoxy resin possess the highest bending stiffness (1389 $N*cm^2$). SBR-impregnated rovings show drastically lower bending stiffness (567 $N*cm^2$), which is in line with their respective applications in the construction industry. While epoxy-impregnated textiles are mainly used for new construction, the more drapable SBR-impregnated textiles are mainly used in retrofitting, where they can be adapted to the shape of the reinforced structure [16]. The water-dispersed epoxy resin achieves comparable bending stiffness (414 $N*cm^2$) to the SBR, while the polycarbonate polyurethane dispersion achieves values (865 $N*cm^2$) in between SBR and epoxy resin. Since the carbon fiber is the same for all coating materials, differences in the bending stiffness of the cured rovings are due to differences in the bending stiffness of the impregnation materials. These results indicate that all four analyzed materials successfully impregnate the carbon roving and achieve bending stiffness values that make them suitable for application as concrete reinforcement.

3.2. Rolling Ball Tests

The development of the tack of the impregnation materials is evaluated using the rolling ball test described above. The change in tack indicates a change in the chemical structure of the impregnation material, meaning that the degree of curing can be assessed by this method. Figure 7 shows the development of the distance traveled by the steel ball over the curing time of the four impregnation materials. A higher distance traveled indicates a lower tack of the materials.
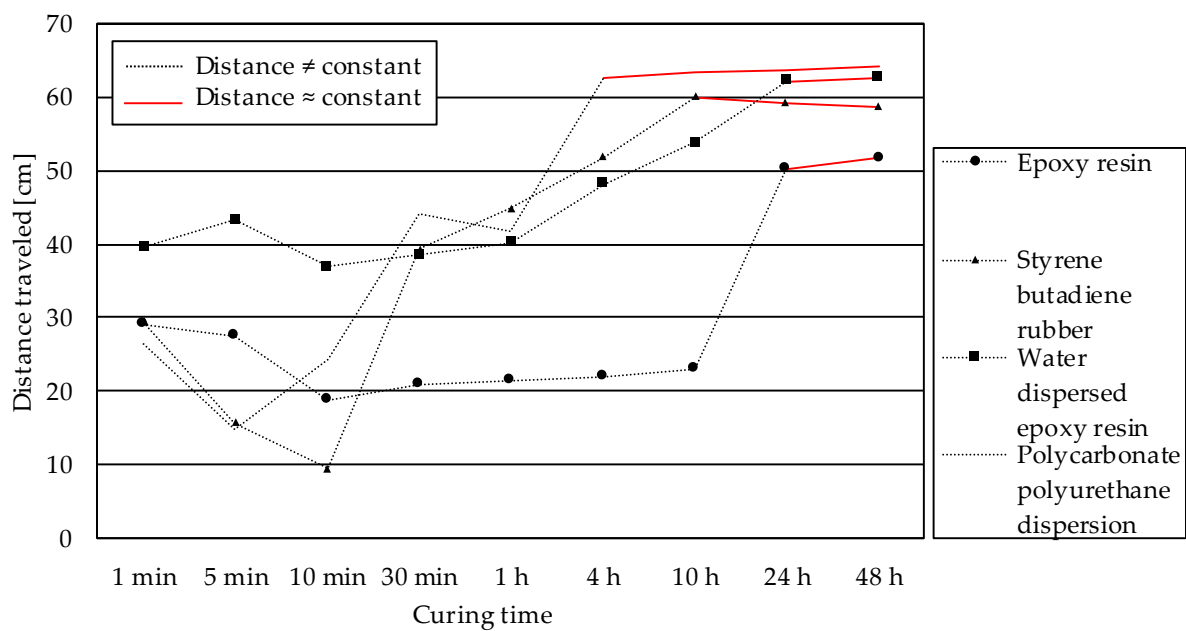
Figure 7. Development of distance traveled by the steel ball across an impregnated textile in the rolling ball test over time.

In general, the development of the distance traveled by the steel ball in the rolling ball test of the curing time follows the same pattern for all materials. Initially, the distance traveled decreases as the tack of the materials increases. Afterward, the distance traveled increases until a plateau is reached and the distance traveled is roughly constant. This constant tack/distance traveled indicates that the chemical reaction within the impregnation material is concluded and the curing process is complete. This happens at different time intervals for the different impregnation materials, with the polycarbonate polyurethane dispersion curing the fastest, reaching its plateau after four hours of curing time. For the SBR impregnation, the plateau is reached after ten hours of curing, while both epoxy-based materials reach their plateaus after 24 h. These values are very relevant for the processing of textiles impregnated with these materials. To ensure a curing within the concrete that improves the fiber matrix bond, textiles must be placed in the concrete matrix prior to the completion of the curing of the impregnation materials. Additionally, any shaping of the textiles within the concrete must also be completed before the curing of the textiles is complete. Based on these results, the time window in which an integration of the prepreg textiles into additive manufacturing processes can be determined in order to be able to produce formable composites with high performance.

3.3. Tensile Tests

To evaluate the mechanical performance of the reinforced concrete, tensile tests on reinforced concrete strips are performed as described above. For each impregnation material, two test series are performed: one in which the impregnation material was cured prior to placing in concrete (fresh-on-hard, FoH) and one in which the impregnation was cured within the concrete matrix (fresh-on-fresh, FoF). The results of the tensile tests are shown in Figure 8 for the FoH specimens and Figure 9 for the FoF specimens. In both figures, the textile stress is calculated by dividing the measured tensile force by the reinforcement area, which is 3.6 mm^2 for all specimens.

Figure 8. Resulting stress–strain curves of all FoH tensile tests: (**a**) epoxy resin; (**b**) styrene butadiene rubber; (**c**) water-dispersed epoxy resin; (**d**) polycarbonate polyurethane dispersion.
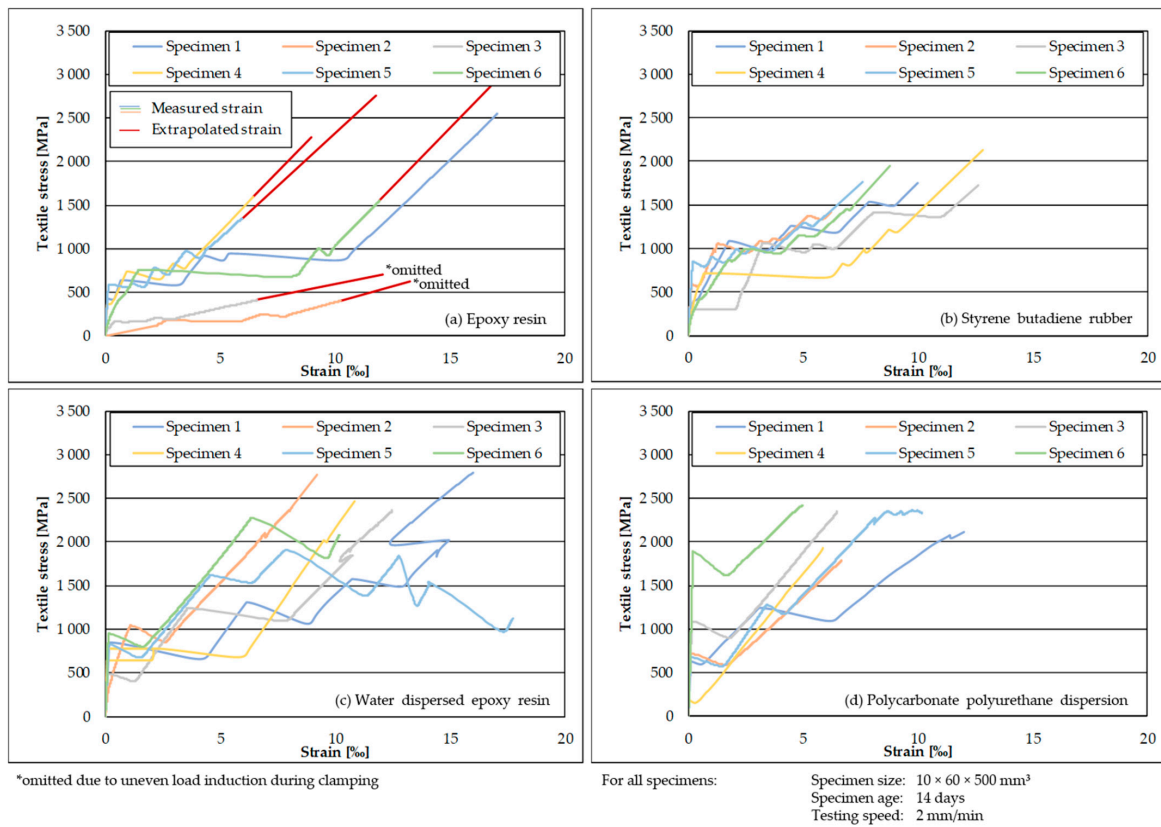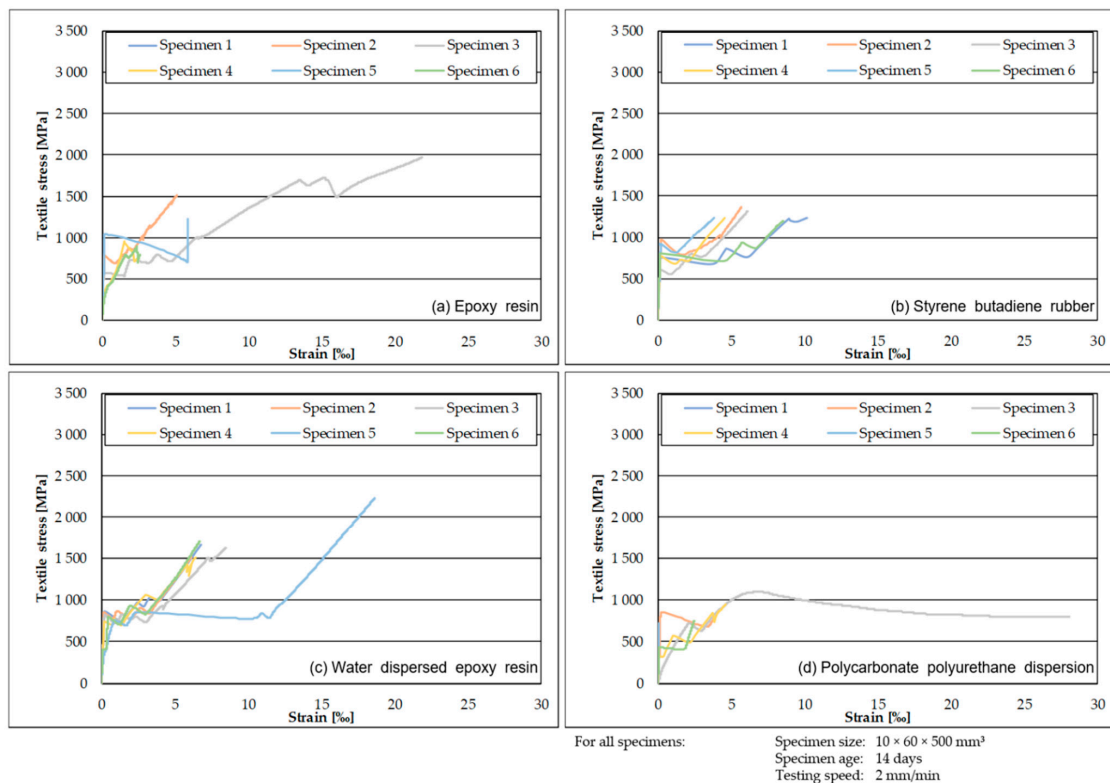

Figure 9. Resulting stress–strain curves of all FoF tensile tests: (**a**) epoxy resin; (**b**) styrene butadiene rubber; (**c**) water-dispersed epoxy resin; (**d**) polycarbonate polyurethane dispersion.

The stress–strain curves of reinforced specimens in Figure 8 with textiles cured prior to insertion into concrete in general follow the expected path as described in [37,38]. Initially, stress increases quickly, until the initial crack develops. Afterward, multiple cracks develop, until the crack formation is concluded and any further strain is carried by the textile reinforcement. The maximum tensile strengths and strains are within a typical range for polymer-impregnated textiles in textile-reinforced concrete. Only the epoxy resin-impregnated series are somewhat below the typical values of 3000–4000 MPa as known from [37,38] which is probably due to the manual impregnation process and the lack of weft rovings. The epoxy resin (ER) and SBR series showed more cracks than the water-dispersed epoxy resin and polycarbonate polyurethane dispersion series.

Thus, the ER and SBR series seem to have a better bond between concrete and impregnated rovings. This multiple cracking is particularly important for use in concrete construction, as it reduces the crack widths of the individual cracks and prevents the ingress of water with potential contaminants such as chlorides.

Especially, the series with polycarbonate polyurethane dispersion does not show a good crack distribution, although the maximum tensile strength is similar to the SBR-impregnated series. The polycarbonate polyurethane dispersion series seems to have a poorer bond to the concrete than the other three series. This effect can also be attributed to the manufacturing effect of the rovings, as they were produced by hand and, therefore, do not have the same dimensional stability as production-scale textiles.

For the epoxy resin-impregnated textiles, the graphs are separated into two sections. Initially, the strain is measured by external strain measurement devices as described above. Since these specimens failed suddenly and violently, these displacement transducers were removed prior to failure to prevent damage. The displacement transducers were removed after completion of crack formation, at which point the stress–strain curve was assumed to be linear and extrapolated based on the measured stress. Another peculiarity of the epoxy-impregnated specimens is that two of the specimens performed significantly worse than the other four. In both specimens, the failure happened in one of the outermost reinforcing rovings, suggesting that the two specimens were not loaded symmetrically and might not have been clamped entirely straight. Therefore, these specimens are omitted from further evaluation.

Similarly to the curves discussed above, the stress–strain curves of reinforced specimens with textiles cured after insertion into concrete in general follow the path as described in [37,38]. All three distinct areas (concrete strain up to the initial crack, multiple crack formation, and textile strain) are present, although the textile strain section is much less pronounced than in the FoH curves. In addition, fewer cracks are formed on average, indicating a lower bond strength between reinforcement and concrete.

As expected, the freshly-impregnated ER series shows that the ER does not cure well in a concrete environment, most likely due to the water content. The water in the concrete has prevented the bond between the concrete and the textile from being as good as that of the FoH series. Moreover, the FoF series has a significantly lower tensile strength. However, this can also be attributed to the manufacturing process, as the rovings were not perfectly aligned despite the clamping during concrete hardening. This effect also applies to the other series.

In the SBR and water-dispersed epoxy resin (FoF) series, the measured deformation during the test is significantly lower than in the (FoH) series. Moreover, the scatter within the series is significantly lower. However, the cracking of the SBR series is significantly worse than that of the FoH series (cf. Table 5), whereas the cracking of the water-dispersed epoxy resin series is much more pronounced. Especially in the water-dispersed epoxy resin series, a pronounced strengthening could be observed in the FoF series compared to the FoH series. The water-dispersed epoxy resin impregnation thus seems to be significantly better suited for the prepreg approach than the other series.

Table 5. Maximum tensile stresses at breaking point for TRC tensile test specimens reinforced with impregnated rovings and the uncoated control.

Impregnation Material	Type of Curing	Average Number of Cracks	Average Maximum Tensile Stress [MPa]	Standard Deviation of Maximum Tensile Stress [MPa]
Epoxy resin	Cured in air (FoH)	4.2	2610	256
	Cured in concrete (FoF)	4.2	1228	445
Styrene-butadiene-rubber dispersion	Cured in air (FoH)	5.2	1791	238
	Cured in concrete (FoF)	3.5	1264	64
Water-dispersed epoxy resin	Cured in air (FoH)	4.2	2430	333
	Cured in concrete (FoF)	4.7	1711	268
Polycarbonate polyurethane dispersion	Cured in air (FoH)	3.2	2159	260
	Cured in concrete (FoF)	2.2	830	180

The stresses at failure are lower for FoF specimens compared to FoH specimens, as shown in Figure 10. In addition, Figure 10 includes the average maximum textile stresses for a control series reinforced with non-impregnated carbon rovings. These are also listed in Table 5.
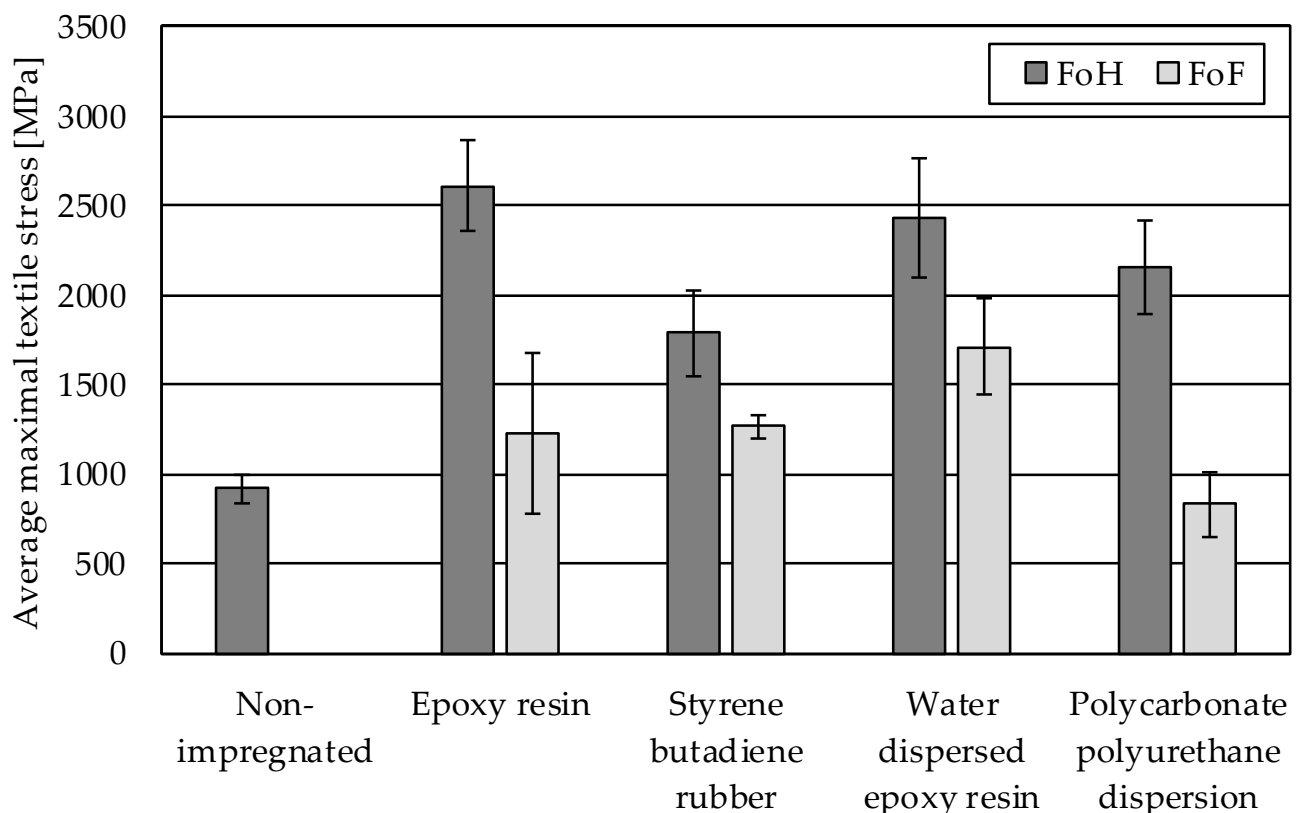
Figure 10. Comparison of the average maximum tensile stresses at breaking point for TRC tensile test specimens reinforced with different impregnated rovings and the uncoated control (error bars indicate standard deviation).

As can be seen in Figure 10 and Table 5, all impregnation materials but the polycarbonate polyurethane dispersion cured within the concrete improve the average maximum tensile stresses compared to the non-impregnated control. Improving maximum

tensile stresses by impregnating the reinforcement textile is in line with the existing literature [14,16] and suggests that the impregnation materials successfully enable load induction into the inner filaments of the rovings. For epoxy resin and styrene butadiene rubber cured prior to placement in concrete (FoH), the obtained values are on the lower end of the literature values obtained in similar tests, e.g., in [37,39,40]. One reason for this lower performance might be the use of rovings and not the finished textiles in this study since the rovings are not placed perfectly parallel to each other and, therefore, not loaded completely evenly. In addition, most literature studies use textiles provided commercially, which are impregnated using industrial processes and not in the laboratory, most likely resulting in a more even impregnation.

As can also be seen in Figure 10, the average maximum tensile stresses reached are lower for all FoF series compared to their respective FoH series, indicating that all curing reactions are inhibited by the concrete environment. This effect is most pronounced for epoxy resin and polycarbonate polyurethane dispersion, where the FoF series only reach 47%/38.4% of the FoH average maximum textile stress, respectively. For styrene butadiene rubber and water-dispersed epoxy resin, the FoF series reach 70.6%/70.4% of the average maximum textile stress of the respective FoH series, suggesting that these materials are less inhibited in their curing reactions by the concrete environment.

These results are not consistent with the results by Dilthey et al. [41], where the pull-off force for the fresh-on-fresh series was always higher than that of the fresh-on-hard series. The main difference was the testing method: where Dilthey et al. only used pull-off tests to evaluate the bond strength between concrete and polymer, we used tensile tests with an embedded roving, which evaluates the composite strength of multiple interfaces (roving–polymer–concrete).

The highest average maximum textile stresses for an FoF series are reached using water-dispersed epoxy resin (1711 MPa), achieving values comparable to FoH styrene butadiene rubber (1791 MPa). Since textiles impregnated with water-dispersed epoxy resin are perfectly drapable prior to curing and more flexible than cured styrene butadiene rubber-impregnated textiles (the current state of the art), water-dispersed epoxy resins are a promising candidate for further investigations.

In the first step, various types of water-dispersed epoxy resins should be compared, to determine which factors influence curing speed and quality within the concrete matrix. However, the results of our study indicate that impregnation with the water-dispersed epoxy resin used here and curing it within concrete enables a perfectly drapable textile with mechanical performance comparable to currently employed SBR textiles. Therefore, the water-dispersed epoxy resin-impregnated textiles can be incorporated into TRC and can be cured within the concrete, enabling the use of such textiles in novel production methods in need of highly drapable textiles with high tensile strength, such as concrete extrusion or 3D concrete printing.

For the other materials analyzed in this study, the approach of curing within concrete leads to comparatively low mechanical performance, since the curing reaction is impeded by the humid and alkaline concrete environment. Further investigations into these materials should focus on facilitating the curing reaction within the concrete, for example by using protective additives or by introducing heat to increase the curing speed.

Additionally, alternative materials cured by the humid and alkaline environment of the concrete might be promising. Furthermore, the analysis of the approach described in this study in conjunction with polymer concrete might provide a fruitful avenue of research. Another aspect that warrants further research is the rheological behavior of the concrete and the impregnation materials, especially in the interface zone.

4. Conclusions

The aim of this work was to develop prepreg polymer-based textiles for use in additive manufacturing methods that can be applied flexibly and, at the same time, exhibit high tensile strength. Within the scope of this study, different polymer impregnation materials for

carbon fibers were analyzed for their curing properties and their mechanical performance when cured within a concrete environment. The results indicate that the humid and alkaline environment of the concrete interferes with the curing reactions of all tested materials. Nevertheless, water-dispersed epoxy resins show an acceptable mechanical performance with a significant formation of cracks and high bonding properties when cured in concrete, indicating that this material class warrants further investigation for the implementation, e.g., in the extrusion or 3D concrete printing processes. The main results obtained in this study are:

- A modified cantilever test based on modeling textiles as a cantilever fixed on one side and measuring the deflection is suitable to compare the bending stiffness of stiff, impregnated textiles.
- A rolling ball test enables the determination of the progress of the curing reaction of impregnation materials, allowing an assessment of the timeframe in which textiles must be placed within the concrete to ensure curing within the concrete matrix.
- Impregnated and cured textile reinforcements significantly improve the tensile strength of reinforced concrete specimens compared to non-impregnated reinforcement. This effect is confirmed for materials reported in the literature (epoxy resin, increase in strength of 185%; styrene butadiene rubber, increase in strength of 95%) as well as novel materials analyzed in this study (water-dispersed epoxy resin, increase in strength of 165%; polycarbonate polyurethane dispersion, increase in strength of 135%).
- For impregnated textiles cured within the concrete, mechanical performance is lower compared to the respective textiles cured prior to insertion into concrete. However, for all materials except polycarbonate polyurethane dispersion, performance is higher than the non-impregnated control (epoxy resin, increase in strength of 34%; styrene butadiene rubber, increase in strength of 38%; water-dispersed epoxy resin, increase in strength of 87%; polycarbonate polyurethane dispersion, loss in strength of 9%).
- Since water-dispersed epoxy resin cured within concrete showed the highest performance of all materials with a significant formation of cracks and high bonding properties cured within concrete (1711 MPa) and achieved similar performance to styrene butadiene rubber cured prior to insertion into concrete (1791 MPa), which is currently used in the industry, this material class warrants further investigation for the integration in additive manufacturing processes like 3D printing and extrusion.

Author Contributions: Conceptualization, M.S., M.K., T.M., M.R. and T.G.; Data curation, M.S. and M.K.; Formal analysis, M.S. and M.K.; Funding acquisition, T.M., M.R. and T.G.; Investigation, M.S. and M.K.; Methodology, M.S. and M.K.; Project administration, T.M., M.R. and T.G.; Resources, M.S., M.K., T.M., M.R. and T.G.; Supervision, T.M., M.R. and T.G.; Validation, M.S. and M.K.; Visualization, M.S. and M.K.; Writing—original draft, M.S.; Writing—review and editing, M.S., M.K., T.M., M.R. and T.G. All authors have read and agreed to the published version of the manuscript.

Institutional Review Board Statement: Not applicable.

Informed Consent Statement: Not applicable.

Data Availability Statement: All relevant data are available in the article and in Appendix A.

Conflicts of Interest: The authors declare no conflict of interest.

Appendix A

Table A1. Measured and calculated data for the cantilever test.

Material	Specimen No.	M	b	l_o	w_{50}	EI	Average EI	Standard Deviation EI
Epoxy resin	1	1360.0	0.50	50	1.8	1544.2	1388.9	149.6
	2	1163.6	0.55	50	1.9	1376.8		
	3	1163.6	0.55	50	2.1	1245.7		
Styrene butadiene rubber	1	1680.0	0.25	50	2.5	686.7	566.6	104.6
	2	1266.7	0.30	50	3.0	517.8		
	3	1142.9	0.35	50	3.3	495.5		
Water-dispersed epoxy resin	1	1700.0	0.20	50	3.1	448.3	414.1	55.3
	2	1520.0	0.25	50	3.5	443.8		
	3	1200.0	0.35	50	4.9	350.4		
Polycarbonate polyurethane dispersion	1	1920.0	0.25	50	2.1	934.3	865.4	130.1
	2	2200.0	0.20	50	1.9	946.6		
	3	1400.0	0.30	50	2.4	715.3		

EI being the bending stiffness in $N*cm^2$, M being the mass per area in g/m^2, b being the specimen width in cm, l_o being the overhang length in cm, and w_{50} being the deflection at the tip of the roving in cm.

References

1. European Commission. On Resource Efficiency Opportunities in the Building Sector. COM(2014) 445 Final, Brussels, 2014. Available online: https://ec.europa.eu/environment/eussd/pdf/SustainableBuildingsCommunication.pdf (accessed on 13 October 2022).
2. European Commission. Communication From the Commission to the European Parliament, the Council, the European Economic and Social Committee and the Committee of the Regions: Roadmap to a Resource Efficient Europe. COM(2011) 571 Final, Brussels, 2011. Available online: https://eur-lex.europa.eu/legal-content/EN/TXT/PDF/?uri=CELEX:52011DC0571&from=EN (accessed on 13 October 2022).
3. Ruuska, A.; Häkkinen, T. Material Efficiency of Building Construction. *Buildings* **2014**, *4*, 266–294. [CrossRef]
4. Beyond Zero Emissions. *Rethinking Cement: Zero Carbon Industry Plan*; Beyond Zero Emissions Inc.: Fitzroy, Australia, 2017; ISBN 978-0-9923580-2-0.
5. Farzampour Alireza. Temperature and humidity effects on behavior of grouts. *Adv. Concr. Constr.* **2017**, *5*, 659–669. [CrossRef]
6. Mansouri, I.; Shahheidari, F.S.; Hashemi, S.M.A.; Farzampour, A. Investigation of steel fiber effects on concrete abrasion resistance. *Adv. Concr. Constr.* **2020**, *9*, 367–374. [CrossRef]
7. Chalangaran, N.; Farzampour, A.; Paslar, N.; Fatemi, H. Experimental investigation of sound transmission loss in concrete containing recycled rubber crumbs. *Adv. Concr. Constr.* **2021**, *11*, 447–454. [CrossRef]
8. Adesina, A. Recent advances in the concrete industry to reduce its carbon dioxide emissions. *Environ. Chall.* **2020**, *1*, 100004. [CrossRef]
9. Bostanci, S.C.; Limbachiya, M.; Kew, H. Use of recycled aggregates for low carbon and cost effective concrete construction. *J. Clean. Prod.* **2018**, *189*, 176–196. [CrossRef]
10. Chalangaran, N.; Farzampour, A.; Paslar, N. Nano Silica and Metakaolin Effects on the Behavior of Concrete Containing Rubber Crumbs. *CivilEng* **2020**, *1*, 264–274. [CrossRef]
11. Watari, T.; Cao, Z.; Hata, S.; Nansai, K. Efficient use of cement and concrete to reduce reliance on supply-side technologies for net-zero emissions. *Nat. Commun.* **2022**, *13*, 4158. [CrossRef]
12. Farzampour, A. Compressive Behavior of Concrete under Environmental Effects. In *Compressive Strength of Concrete*; Kryvenko, P., Ed.; IntechOpen: London, UK, 2020; ISBN 978-1-78985-567-8.
13. Peled, A.; Bentur, A.; Mobasher, B. *Textile Reinforced Concrete*; CRC Press: London, UK, 2017; ISBN 9781315119151.
14. Hegger, J.; Voss, S. Investigations on the bearing behaviour and application potential of textile reinforced concrete. *Eng. Struct.* **2008**, *30*, 2050–2056. [CrossRef]
15. Koutas, L.N.; Tetta, Z.; Bournas, D.A.; Triantafillou, T.C. Strengthening of Concrete Structures with Textile Reinforced Mortars: State-of-the-Art Review. *J. Compos. Constr.* **2019**, *23*, 3118001. [CrossRef]
16. Friese, D.; Scheurer, M.; Hahn, L.; Gries, T.; Cherif, C. Textile reinforcement structures for concrete construction applications——a review. *J. Compos. Mater.* **2022**, *56*, 002199832211271. [CrossRef]
17. Laiblová, L.; Pešta, J.; Kumar, A.; Hájek, P.; Fiala, C.; Vlach, T.; Kočí, V. Environmental Impact of Textile Reinforced Concrete Facades Compared to Conventional Solutions-LCA Case Study. *Materials* **2019**, *12*, 3194. [CrossRef]

18. Scope, C.; Guenther, E.; Schütz, J.; Mielecke, T.; Mündecke, E.; Schultze, K.; Saling, P. Aiming for life cycle sustainability assessment of cement-based composites: A trend study for wall systems of carbon concrete: Dresden Nexus Conference 2020-Session 4-Circular economy for building with secondary construction materials to minimise resource use and land use. *Civ. Eng. Des.* **2020**, *2*, 143–158. [CrossRef]

19. Stoiber, N.; Hammerl, M.; Kromoser, B. Cradle-to-gate life cycle assessment of CFRP reinforcement for concrete structures: Calculation basis and exemplary application. *J. Clean Prod.* **2021**, *280*, 124300. [CrossRef]

20. Curbach, M.; Jesse, F. Eigenschaften und Anwendung von Textilbeton. *Beton-Und Stahlbetonbau* **2009**, *104*, 9–16. [CrossRef]

21. *Textile Fibre Composites in Civil Engineering*; Triantafillou, T. (Ed.) Elsevier: Amsterdam, The Netherlands, 2016; ISBN 9781782424468.

22. Mechtcherine, V.; Michel, A.; Liebscher, M.; Schneider, K.; Großmann, C. Mineral-impregnated carbon fiber composites as novel reinforcement for concrete construction: Material and automation perspectives. *Autom. Constr.* **2020**, *110*, 103002. [CrossRef]

23. Nadiv, R.; Peled, A.; Mechtcherine, V.; Hempel, S.; Schroefl, C. Micro- and nanoparticle mineral coating for enhanced properties of carbon multifilament yarn cement-based composites. *Compos. Part B Eng.* **2017**, *111*, 179–189. [CrossRef]

24. Schneider, K.; Lieboldt, M.; Liebscher, M.; Fröhlich, M.; Hempel, S.; Butler, M.; Schröfl, C.; Mechtcherine, V. Mineral-Based Coating of Plasma-Treated Carbon Fibre Rovings for Carbon Concrete Composites with Enhanced Mechanical Performance. *Materials* **2017**, *10*, 360. [CrossRef]

25. Raoof, S.M.; Koutas, L.N.; Bournas, D.A. Bond between textile-reinforced mortar (TRM) and concrete substrates: Experimental investigation. *Compos. Part B Eng.* **2016**, *98*, 350–361. [CrossRef]

26. Glowania, M.; Gries, T.; Schoene, J.; Schleser, M.; Reisgen, U. Innovative Coating Technology for Textile Reinforcements of Concrete Applications. *KEM* **2011**, *466*, 167–173. [CrossRef]

27. Beckmann, B.; Bielak, J.; Bosbach, S.; Scheerer, S.; Schmidt, C.; Hegger, J.; Curbach, M. Collaborative research on carbon reinforced concrete structures in the CRC/TRR 280 project. *Civ. Eng. Des.* **2021**, *3*, 99–109. [CrossRef]

28. Mechtcherine, V.; Michel, A.; Liebscher, M.; Schmeier, T. Extrusion-Based Additive Manufacturing with Carbon Reinforced Concrete: Concept and Feasibility Study. *Materials* **2020**, *13*, 2568. [CrossRef] [PubMed]

29. Bos, F.P.; Lucas, S.S.; Wolfs, R.J.; Salet, T.A. (Eds.) *Second RILEM International Conference on Concrete and Digital Fabrication*; Springer International Publishing: Cham, Switzerland, 2020; ISBN 978-3-030-49915-0.

30. Kalthoff, M.; Raupach, M.; Matschei, T. Investigation into the Integration of Impregnated Glass and Carbon Textiles in a Laboratory Mortar Extruder (LabMorTex). *Materials* **2021**, *14*, 7406. [CrossRef] [PubMed]

31. Kalthoff, M.; Raupach, M.; Matschei, T. Extrusion and Subsequent Transformation of Textile-Reinforced Mortar Components—Requirements on the Textile, Mortar and Process Parameters with a Laboratory Mortar Extruder (LabMorTex). *Buildings* **2022**, *12*, 726. [CrossRef]

32. Teijin Carbon Europe GmbH. Tenax Filament Yarn Product Data Sheet. Available online: https://www.teijincarbon.com/fileadmin/PDF/Datenbl%C3%A4tter_dt/Product_Data_Sheet_TSG01de__EU_Filament___DE_.pdf (accessed on 13 October 2022).

33. *DIN 53362:2003-10*; Testing of Plastics Films and Textile Fabrics (Excluding Nonwovens), Coated or not Coated Fabrics–Determination of Stiffness in Bending–Method According to Cantilever. Beuth Verlag GmbH: Berlin, Germany, 2003. [CrossRef]

34. Duncan, B.C.; Lay, L. An Intercomparison of Tack Measurements. NPL Report, Teddington. 1999. Available online: http://eprintspublications.npl.co.uk/1246/ (accessed on 1 December 2022).

35. D10 Committee. *Test Method for Tack of Pressure-Sensitive Adhesives by Rolling Ball*; ASTM International: West Conshohocken, PA, USA, 2007. [CrossRef]

36. Recommendation of RILEM TC 232-TDT: Test methods and design of textile reinforced concrete. *Mater. Struct.* **2016**, *49*, 4923–4927. [CrossRef]

37. Bielak, J. Shear in Slabs with Non-Metallic. Reinforcement. Dissertation, RWTH Aachen University, Aachen, Germany, 2021. [CrossRef]

38. Morales Cruz, C. Crack-Distributing Carbon Textile Reinforced Concrete Protection Layers. Dissertation, RWTH Aachen University, Aachen, Germany, 2020. [CrossRef]

39. Kulas, C. Load-Bearing Behavior of Impregnated Textile Reinforcements for Concrete Members. Dissertation, RWTH Aachen University, Aachen, Germany, 2014.

40. Carozzi, F.G.; Poggi, C. Mechanical properties and debonding strength of Fabric Reinforced Cementitious Matrix (FRCM) systems for masonry strengthening. *Compos. Part B Eng.* **2015**, *70*, 215–230. [CrossRef]

41. Dilthey, U.; Schleser, M.; Puterman, M. Investigation and improvement of concrete reinforced with epoxy impregnated fabrics. In *Proceedings of the 12th International Congress 'Polymers in Concrete', ICPIC 07, Chuncheon, Korea, 26–28 September 2007*; Yeon, K.-S., Ed.; Kangwoon National University: Chancheon, Republic of Korea, 2007.